International Journal of Remote Sensing
Vol. 29, No. 19, 10 October 2008, 5605–5622

Taylor & Francis
Taylor & Francis Group

Extracting forest canopy structure from spatial information of high resolution optical imagery: tree crown size versus leaf area index

C. SONG*† and M. B. DICKINSON‡
†Department of Geography, CB# 3220, 205 Saunders Hall, University of North Carolina at Chapel Hill, Chapel Hill, NC, USA
‡US Forest Service, Northern Research Station, 359 Main Road, Delaware, OH 43015, USA

(*Received 1 December 2006; in final form 10 March 2008*)

Leaves are the primary interface where energy, water and carbon exchanges occur between the forest ecosystems and the atmosphere. Leaf area index (LAI) is a measure of the amount of leaf area in a stand, and the tree crown size characterizes how leaves are clumped in the canopy. Both LAI and tree crown size are of essential ecological and management value. There is a lot of interest in extracting both canopy structural parameters from remote sensing. The LAI is generally estimated with spectral information from remotely sensed images at relatively coarse spatial resolution. There has been much less success in estimating tree crown size with remote sensing. The recent availability of abundant high spatial resolution imagery from space offers new potential for extracting LAI and tree crown size, particularly in the spatial domain. This study found that the spatial information in Ikonos imagery is highly valuable in estimating both tree crown size and LAI. When the conifer- and hardwood-dominated stands are pooled, tree crown sizes of conifer stands relate best to the ratio of image variance at 2×2 m spatial resolution to that at 3×3 m spatial resolution, while LAI relates best to image variance at 4×4 m spatial resolution. When the conifer- and hardwood-dominated stands are separated, image spatial information estimates tree crown size much better for conifer-dominated stands than for the hardwood-dominated stands, while the relationship between image spatial information and LAI is strengthened after the two types of stands are combined. Tree crown size is more sensitive to image spatial resolution than LAI. Image variance is more useful in estimating LAI than normalized difference vegetation index (NDVI) and simple ratio vegetation index (SRVI). Combining both spatial and spectral information provides some improvement in estimating LAI compared with using spatial information alone. Therefore, future efforts to estimate canopy structure with high resolution imagery should also use image spatial information.

1. Introduction

Leaves are the primary interface where energy, water, and carbon exchanges occur between forest ecosystems and the atmosphere. The amount of leaf area in a stand is a crucial structural parameter. The amount of leaf area in a forest stand is usually measured by leaf area index (LAI), which is defined as the ratio of one-sided leaf areas in a stand to the ground area it occupies (Monteith and Unsworth 1973). For

*Corresponding author. Email: csong@email.unc.edu

International Journal of Remote Sensing
ISSN 0143-1161 print/ISSN 1366-5901 online © 2008 Taylor & Francis
http://www.tandf.co.uk/journals
DOI: 10.1080/01431160802060904

conifer species, the projected leaf areas are generally used in calculating LAI (Barclay and Goodman 2000). It is extremely laborious and costly, and usually impractical, to estimate LAI in the field through direct measurement by destructive sampling. Therefore, numerous optical instruments have been developed to estimate LAI indirectly (Gower and Norman 1991, Welles and Norman 1991, Chen *et al.* 1997). Although using these optical instruments to estimate LAI saves much effort compared to destructive sampling, it remains a laborious process, and is impractical to estimate LAI at the landscape scale.

Remote sensing has been deemed as the only viable option to obtain a continuous LAI surface over large areas. Although algorithms have been developed to map LAI from local (Welles and Norman 1991, Chen and Cihlar 1996) to global scales (Knyazikhin *et al.* 1998, Myneni *et al.* 2002), rigorous validation efforts found that significant errors may exist in existing LAI products (Cohen *et al.* 2003). The recent availability of high resolution optical imagery offers new potential in estimating LAI from remote sensing. Past efforts have focused primarily on the spectral signals (Chen and Cihlar 1996, White *et al.* 1997, Turner *et al.* 1999, Peddle *et al.* 2001, Stenberg *et al.* 2004). The potential of using the spatial information in high resolution imagery for extracting LAI has not been fully investigated. Previous studies found that window-based image texture improved the retrieval of LAI in combination with spectral vegetation indices (Wulder *et al.* 1998, Colombo *et al.* 2003). It is not clear how well image spatial information alone relates to LAI at a stand scale.

The exchanges of energy, water and carbon between forest ecosystems and the atmosphere are not only determined by the amount of leaves in the canopy, but are also strongly influenced by how the leaves are arranged. Leaves in the canopy are often clumped at multiple scales from shoots to whorls, branches and crowns (Ni *et al.* 1997). However, crowns are the most important scale with respect to energy interception (Kucharich *et al.* 1999), hence carbon assimilation and transpiration in the canopy.

Measuring tree crown size is also very laborious, and it is nearly impossible to obtain a tree crown size map over the landscape via direct measurements in the field. Estimating tree crown size with remote sensing proved to be difficult before the advent of space-borne high resolution optical imagery because there is little relationship between spectral signature and tree size. Furthermore, spatial resolution of the remotely sensed imagery from space is too coarse (Cohen *et al.* 1995). Franklin and Strahler (1988) and Wu and Strahler (1994) did have some success in using the Li–Strahler model (Li and Strahler 1985) for estimating tree size and cover with Landsat TM imagery. Woodcock *et al.* (1994, 1997) also found that Landsat TM imagery can be used to map tree cover, but to separate tree cover into tree crown size and density was difficult. With the advent of high spatial resolution optical imagery from space, there is now great potential for mapping many forest biophysical parameters (Franklin *et al.* 2001, Asner *et al.* 2002, Hurrt *et al.* 2003, Clark *et al.* 2004, Kayitakire *et al.* 2006). Based on the theory of the disc scene model (Jupp *et al.* 1988, 1989), Song and Woodcock (2003) developed an analytical model that directly links scene structure to the spatial properties of multiple resolution imagery. The theory has proved effective in retrieving tree crown size, particularly for conifer stands (Song 2007).

The objective of this study is to further investigate how well image spatial information at the stand scale can be used to retrieve tree crown size and LAI for

forested landscapes and how the relationships between image spatial information and both tree crown size and LAI differ. Tree crown size and LAI are critical canopy structure parameters that are highly valuable in forest ecology and management. They can be used directly as model input to simulate canopy processes (Ni *et al.* 1997, Song and Band 2004). An improved LAI product could also be used to calibrate LAI products derived from imagery with coarser spatial resolution.

2. Methodologies

2.1 *Field data collection*

The study area is located in the Blackwood Division of Duke Forest (35°58′42″ N, 79°05′39″ W) and surrounding areas in the Piedmont region of North Carolina. The local terrain is relatively flat (<5% slope). Conifer species are dominated by loblolly pine (*Pinus taeda*). The hardwood stands are dominated by white oak (*Quercus alba*), red oak (*Quercus rubra*), sweet gum (*Liquidambar styraciflua*), red maple (*Acer rubrum*), yellow popular (*Liriodendron tulipifera*) and hickory (*Carya ovata*).

The objectives of the fieldwork were to estimate the mean tree crown size and LAI for the stands sampled. Twenty-one circular plots with variable diameters were established during late spring and early summer of 2005. The default plot diameter was 30 m, but the size was increased for stands with fewer large trees, and decreased for stands with many small trees so that the sampling plot was representative of the stand. The plots were established in the middle of relatively large and uniform stands. The average plot attributes were assumed representative of the stand. The centre location of each plot was recorded with a Garmin 12XL GPS receiver. After the centre of a plot was located, the plot boundary was identified with flagging tape. All trees around the edge were marked whether they were inside or outside the plot. The diameter at breast height (DBH) of each individual tree greater than 2.5 cm was measured and its species was recorded. Repeat measurements were avoided by marking stems with chalk. The tree crown diameter (CD) was measured in two orthogonal directions (one along the maximum width) with fibreglass tapes. The average CD in the two directions is used to represent the tree crown size.

For each plot, a minimum of 16 individuals, uniformly distributed within the range of the DBH of the plot, were selected for crown diameter measurements. At the end of the fieldwork, all the tree crown measurements from all plots were pooled and sorted by species. The allometric relationship was developed on a species-specific basis. The following species-specific allometric relationship between DBH and CD was assumed:

$$\ln Y = b_0 + b_1 \ln X, \tag{1}$$

where b_0 and b_1 are constants, the independent variable (X) is the DBH, and the dependent variable (Y) is the CD. The tree crown sizes for the individuals that were not measured in the field were then calculated by species using equation (1). After the CD was calculated for each individual within a plot, the mean crown diameter of the plot was calculated as:

$$\overline{D} = \sqrt{\frac{\sum_{i=1}^{n} D_i^2}{n}}, \tag{2}$$

where D_i is the CD of a given individual within a plot, $\bar{D}$ is the mean CD of the plot and n is the number of trees within the plot.

The LAI for the sample stands was estimated from the DBH and species-specific allometric relationships from a comprehensive database compiled by the US Forest Service (Jenkins *et al.* 2004). The allometric relationships were first used to calculate leaf biomass for each individual. The biomass was then converted to leaf area, based on the generalized specific leaf area for temperate evergreen needle-leaf trees and temperate deciduous broad-leaf trees used in Biome-BGC (Running and Hunt 1993, Thornton 2000). The leaf area index for each plot was calculated as:

$$\mathrm{LAI} = \frac{\sum_{i=1}^{n} A_i}{\pi D^2/4}, \tag{3}$$

where A_i is the leaf area for an individual tree, D is the diameter of the circular plot and n is the number of trees in the plot.

As a comparison, LAI was also measured with LAI-2000 for 11 of the 21 plots. Due to constraints of accessibility and sky conditions, LAI could not be measured with the instrument for every sampled stand. The 90° viewing cap was applied to the optical sensor to minimize the influences of the operator and surrounding objects. For each sample plot, an 'above' canopy measurement was taken in a nearby open area before and after measurements inside the canopy. For each plot, we took five measurements under the canopy: one in the plot centre and one in the middle of the radius in four orthogonal directions. Due to varying mixtures of broad leaf and coniferous trees, it is quite difficult to adjust for the clumping effect from LAI-2000 measurements. Thus, LAI estimated with LAI-2000 is only used for comparative purposes.

2.2 *Remotely sensed data*

All sampled plots were located within the scope of a remotely sensed image from the Ikonos satellite collected on 23 September 2004 with the Blackwood Division of Duke Forest at the centre of the image. The image covered an area of 10×10 km. The sun elevation and azimuth angles at the time of image acquisition were 59.0° and 159.9°, respectively. The cloud cover in the image is zero. For each sampling plot, a polygon was drawn on the Ikonos image that enclosed the entire stand. The digital numbers (DNs) from the panchromatic image were used for spatial analyses. The multispectral images in the red and near-infrared bands were used to calculate vegetation indices. Because of the linear relationship between the surface reflectance and DNs, the raw DNs can be used for spatial analysis. However, because the relationships between vegetation indices and surface reflectance are nonlinear, the multispectral images need to be converted to reflectance values. Since we lacked the *in situ* atmospheric data for retrieval of surface reflectance, we converted the multispectral images into at-satellite reflectance using the approach by Song (2004).

2.3 *Image spatial properties*

Image spatial properties refer to the spatial arrangement of digital numbers. Since each brightness value in a remote sensing image is tied to the location of a pixel, it can be treated as a regionalized variable, and a remote sensing image can be treated as the realization of a spatial function in the space. Therefore, the semivariogram

method of geostatistics can be used to study the spatial pattern of remotely sensed imagery. In this study, our analysis of image spatial properties is based on the disc scene model (Jupp *et al.* 1988, 1989), where the scene of a forest stand is treated as discs randomly distributed on a contrasting background. The discs can overlap, but the brightness value of the overlapped area does not change. Although simple, the model is not unrealistic for a stand viewed from above. The semivariance of a remotely sensed image of an unbounded forest landscape with spatial resolution Z can be written as (Jupp *et al.* 1988):

$$\gamma_Z(h) = C_Z - \mathrm{cov}_Z(h), \tag{4}$$

where C_Z is the sill of the semivariogram for the image and is equivalent to image variance, $\mathrm{cov}_Z(h)$ is the covariance of the brightness value of the remotely sensed image and h is the lag in space. According to Jupp *et al.* (1988, 1989):

$$C_Z = 8\int_0^1 tT(t)\mathrm{cov}\left(D_\mathrm{p}, t\right)\mathrm{d}t, \tag{5}$$

and

$$\mathrm{cov}_Z(s) = \frac{8}{\pi}\int_0^s t\Phi(t, s)\mathrm{cov}\left(D_\mathrm{p}, t\right)\mathrm{d}t, \tag{6}$$

where $\mathrm{cov}(D_\mathrm{p}, t)$ is the spatial covariance of the DNs with D_p as the diameter of the sensor instantaneous field of view (IFOV) and t is the integrative variable for standardized distance with respect to the disc, $s=h/D_\mathrm{o}$. The parameter $T(s)$ is the overlap function between the disc with respect to the lag h and is defined as the proportion of overlap for a disc of size D_o as it moves in space:

$$T(s) = \begin{cases} 1 & h = 0, \\ \dfrac{1}{\pi}(\theta - \sin\theta) & h < D_\mathrm{o}, , \\ 0 & h \geq D_\mathrm{o}, \end{cases} \tag{7}$$

where the parameter θ is related to s as $\cos(\theta/2)=s$. It holds that $\mathrm{cov}_Z(h)=0$ when $h>D_\mathrm{o}$ and $\mathrm{cov}_Z(h)=C_Z$ when $h=0$. The parameter $\Phi(t, s)$ in equation (6) integrates the overlap function for discs over azimuth from 0 to π. Song and Woodcock (2003) derived:

$$C_Z = 8(g_\mathrm{D} - g_\mathrm{B})^2 Q^2 \int_0^1 tT(t)\left(\mathrm{e}^{\lambda AT\left(tD_\mathrm{p}/D_\mathrm{o}\right)} - 1\right)\mathrm{d}t, \tag{8}$$

where g_D and g_B are the disc and background brightness values, respectively. $\mathrm{T}(\cdot)$ is the overlap function, as defined in equation (7). The area of the disc is A and the density of the disc is λ. The fraction of the background not covered by the disc is $Q=\exp(-\lambda A)$. A standardized distance for the IFOV (t) in space translates to t $D_\mathrm{p}/D_\mathrm{o}$ as the standardized distance for the disc. Equation (8) directly relates the sill of the regularized image variogram to the scene structure, the size and density of the objects, and the contrast between the disc and the background at a given size of IFOV (D_p). Due to the fact that the contrast between the disc and the background

does not change with the size of the IFOV, the ratio of the sill of the regularized variogram at one spatial resolution to that at another spatial resolution would be solely determined by the scene structure as:

$$\frac{C_{Z1}}{C_{Z2}} = \frac{\int_0^1 tT(t)\left(e^{\lambda AT\left(tD_{p1}/D_o\right)} - 1\right)dt}{\int_0^1 tT(t)\left(e^{\lambda AT\left(tD_{p2}/D_o\right)} - 1\right)dt}, \quad (9)$$

where C_{Z1} and C_{Z2} are the sills of the image variogram with the diameter of the IFOV being D_{p1} and D_{p2}, respectively. Equation (9) is derived from the ratio of equation (8) at two spatial resolutions. Due to the fact that g_D, g_B and Q in equation (8) are independent of spatial resolution, they get cancelled in equation (9). Equation (9) provides the theoretical relationship between the ratio of the sill of image variograms at two spatial resolutions with scene structure, disc size (D_o) and density (λ). In this study, we examined the relationship of tree crown size and LAI with equation (9). We also examined the relationships between canopy structure and image variance across different image spatial resolutions. The Ikonos panchromatic image degraded to a series of coarser spatial resolutions through simple averaging.

3. Results and discussions

3.1 *Tree crown size and LAI*

The species-specific allometric relationship between the CD and the DBH developed in this study is given in table 1. The number of samples for each species in table 1 reflects the abundance of the species in the stands sampled. The coefficient of determination (R^2) for most species is above 0.7, except for red oak (*Quercus rubra*) and sweet gum (*Liquidambar styraciflua*), which have significant variations in the CD for a given DBH. The species in the 'others' category in table 1 were not encountered commonly enough to develop a species specific allometric relationship. These species were pooled together to develop a single allometric relationship. The allometric relationships in table 1 are then applied to all other individuals in the plots to calculate mean tree crown size (see table 2).

The LAI estimated from the allometric relationships (table 2) is highly correlated to the effective LAI estimated independently with LAI-2000 (figure 1). However, the

Table 1. Species-specific allometry between diameter at breast height (DBH) and crown diameter (CD): ln (CD)=b_0+b_1 ln (DBH). The data were collected in the Duke Forest and surrounding areas during late spring and early summer of 2005.

Species	b_0	b_1	R^2	n
Loblolly pine	−1.1013	1.0201	0.7673	103
Shortleaf pine	−0.5554	0.9123	0.8239	15
Hickory	0.0707	0.8617	0.8098	7
Red maple	0.2572	0.7841	0.7361	20
Sweet gum	0.0661	0.7168	0.5454	28
Tulip popular	0.1720	0.6296	0.8348	29
Red oak	0.2335	0.7056	0.5643	8
White oak	−0.0438	0.8185	0.8133	15
Others	0.4882	0.6028	0.5846	13

Table 2. Canopy structure for each sample plot. The mixture of conifer and hardwoods for the individuals in each plot is characterized by the percent basal area of conifers. The average size of the individuals is indicated by the quadratic mean of the DBH.

Plot no.	Basal area conifer (%)	Plot diameter (m)	Stem density (trees ha^{-1})	Quadratic mean DBH (cm)	Plot LAI	Mean CD (m)
1	86.7	30	1995	17.56	5.12	3.21
2	80.9	30	806	25.78	8.28	4.86
3	92.0	30	2080	16.93	4.09	2.92
4	92.2	30	1811	18.22	3.98	2.99
5	17.2	30	566	28.50	8.32	6.33
6	98.1	30	1500	19.90	3.63	2.94
7	83.3	30	1712	18.59	6.48	3.22
8	9.8	30	608	24.96	8.71	5.99
9	0.0	30	3240	9.82	7.18	3.13
10	38.5	30	905	23.46	9.67	5.41
11	26.9	15	8715	6.04	5.67	1.83
12	0.0	40	668	21.24	6.23	4.98
13	51.9	30	920	23.95	9.17	5.01
14	10.5	40	613	28.61	11.72	5.01
15	100.0	20	1974	15.42	3.66	2.88
16	88.6	30	1160	23.35	7.25	4.61
17	87.6	30	1075	22.73	5.51	4.38
18	76.1	30	1174	19.21	6.20	5.35
19	92.5	30	495	26.69	3.33	5.50
20	87.8	30	1146	21.37	4.74	4.06
21	86.3	30	1203	20.57	4.96	3.41

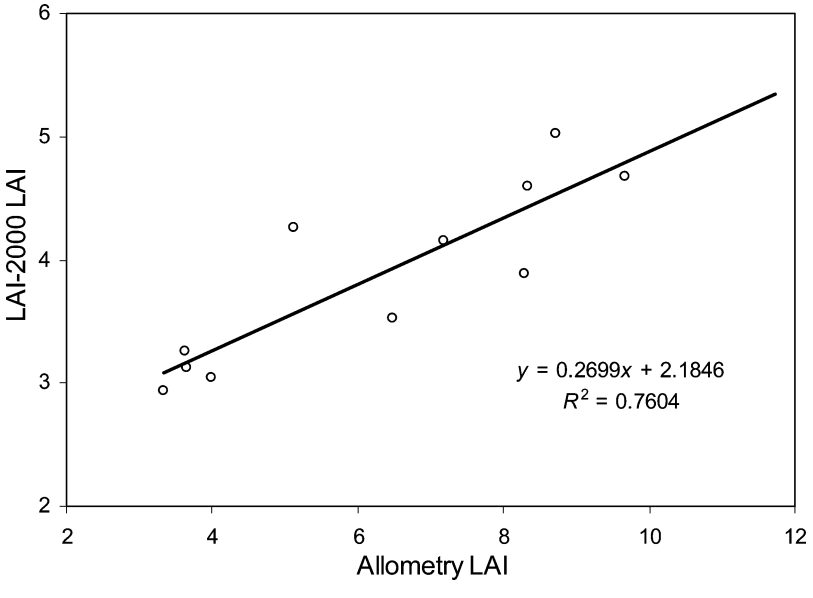

Figure 1. The relationship between effective LAI measured by LAI-2000 and LAI estimated from allometry. The strong relationship indicates that the LAI estimated from allometry is consistent among stands.

LAI estimated by LAI-2000 is significantly lower than those based on allometry. The strong relationship in figure 1 indicates that LAI estimated from allometry is consistent across the stands, although it might be overestimated (Burton *et al.* 1991). As long as the LAI estimate is consistent among the stands sampled, the subsequent analysis is valid.

3.2 *Relationships of tree crown size and LAI with image spatial properties*

The relationships between mean stand tree crown size and image variance at different spatial resolutions are given in table 3. There is a strong relationship between mean tree crown size and image variance for conifers, while the relationship is not significant for hardwoods. When the conifer and hardwood stands are pooled, the relationship is still significant, but the strength of the relationship decreases substantially compared with conifer alone. The weak relationship for hardwoods may result from the more continuous canopy structure in hardwood stands, making individual crowns hard to separate from above.

It is interesting to note that the R^2 for the relationship between mean tree crown size and image variance is not highest at the finest spatial resolution, but peaks at 4×4 m spatial resolution for the stands in this study. Tree crown diameters are usually much larger than 1 m, therefore, the image variance at the highest spatial resolution contains within-crown variance. As pixel size increases to about the average tree crown size, the image variance reflects the difference in tree crown size. This is similar to the scale effect on local variance found by Woodcock and Strahler (1987).

Similar to results shown in table 3, the relationship between mean tree crown size and the ratio of image variances at two spatial resolutions is stronger for conifers than for hardwoods (table 4). When the conifers and hardwoods are pooled, the R^2

Table 3. Results of regression analyses between stand mean tree crown size and image variances at different spatial resolutions. The regression equation is $CD = b_0 + b_1 C_{Zi}$, where C_{Zi} is the image variance at i m spatial resolution.

Image variance	R^2	P value
Conifers		
C_{Z1}	0.2880	0.0586
C_{Z2}	0.5175	0.0056
C_{Z3}	0.6127	0.0016
C_{Z4}	0.6214	0.0014
C_{Z5}	0.5689	0.0029
C_{Z6}	0.5735	0.0037
Hardwoods		
C_{Z1}	0.0930	0.4627
C_{Z2}	0.1569	0.3313
C_{Z3}	0.2134	0.2492
C_{Z4}	0.2227	0.2377
C_{Z5}	0.2212	0.2396
Conifers and hardwoods		
C_{Z1}	0.2296	0.0282
C_{Z2}	0.3003	0.0103
C_{Z3}	0.3394	0.0057
C_{Z4}	0.3417	0.0056
C_{Z5}	0.3366	0.0062
C_{Z6}	0.2983	0.0110

Table 4. Results of regression analyses between stand mean tree crown size and the ratio of image variances at two spatial resolutions. The regression equation is $CD=b_0+b_1R_{ij}$, where R_{ij} is the ratio of image variance at i m spatial resolution to that at j m spatial resolution.

Variance ratio	R^2	P value
Conifers		
R_{12}	0.6175	0.0015
R_{23}	0.7282	0.0002
R_{34}	0.3601	0.0301
R_{45}	0.0535	0.4473
R_{56}	0.0513	0.4566
R_{67}	0.0511	0.4579
Hardwoods		
R_{12}	0.3053	0.1555
R_{23}	0.4723	0.0597
R_{34}	0.3802	0.1035
R_{45}	0.3467	0.1246
R_{56}	0.3206	0.1434
R_{67}	0.0868	0.4787
Conifers and hardwoods		
R_{12}	0.4069	0.0018
R_{23}	0.4765	0.0005
R_{34}	0.3479	0.0048
R_{45}	0.1662	0.0672
R_{56}	0.0095	0.6695
R_{67}	0.0754	0.2367

value is much lower than the R^2 value for conifer stands alone, and slightly higher than the R^2 value for hardwoods. The strongest relationship is for the ratio of image variances at 2 and 3 m spatial resolutions. The relationships between mean crown size and image variance ratios are much stronger than the relationships with image variance at a single spatial resolution in table 3. However, the R^2 values for image variance ratios decrease much faster as pixel sizes increase than do those for image variance at a single spatial resolution.

Table 5 shows the relationship of LAI with image variance at a single spatial resolution. The pattern of R^2 with spatial resolution in table 5 is similar to that in table 3, i.e. the greatest R^2 does not occur at the highest spatial resolution, but at 4×4 m spatial resolution. For conifers, the sensitivity of R^2 in table 5 to changes in spatial resolution is much lower than that in table 3. The R^2 values vary between 0.29 and 0.62 for regression of conifer tree crown size with image variance for spatial resolution of 1×1 m to 6×6 m, while the R^2 values vary between 0.37 and 0.45 for regression of conifer LAI with image variances at the same spatial resolutions. Thus, tree crown size is nearly four times more sensitive than LAI to image spatial resolution with respect to their relationship to image variances. Such a difference in sensitivity to image spatial resolution for tree crown size and LAI is not seen for hardwoods. Unlike the relationships between mean tree crown size and image variance in table 3, the relationship between LAI and image variance at single spatial resolution improved considerably when the conifer- and hardwood-dominated stands were pooled.

The relationship between LAI and the ratio of image variances at two spatial resolutions is shown in table 6. The pattern of R^2 with spatial resolution in table 6 is similar to that in table 4. The highest R^2 value for conifer LAI occurs at the ratio of

Table 5. Results of regression analyses between LAI and image variances at different spatial resolutions. The regression equation is $LAI = b_0 + b_1 C_{Zi}$, where C_{Zi} is the image variance at i m spatial resolution.

Image variance	R^2	P value
Conifers		
C_{Z1}	0.3665	0.0218
C_{Z2}	0.4252	0.0115
C_{Z3}	0.4372	0.0100
C_{Z4}	0.4542	0.0082
C_{Z5}	0.4099	0.0136
C_{Z6}	0.4393	0.0098
Hardwoods		
C_{Z1}	0.2670	0.2350
C_{Z2}	0.3041	0.1994
C_{Z3}	0.3520	0.1602
C_{Z4}	0.3371	0.1717
C_{Z5}	0.3895	0.1341
C_{Z6}	0.3002	0.2029
Conifers and hardwoods		
C_{Z1}	0.5438	0.0001
C_{Z2}	0.5831	0.0001
C_{Z3}	0.6018	0.0001
C_{Z4}	0.6066	0.0001
C_{Z5}	0.6036	0.0001
C_{Z6}	0.5933	0.0001

Table 6. Results of regression analyses between LAI and the ratio of image variances at two spatial resolutions. The regression equation is $LAI = b_0 + b_1 R_{ij}$, where R_{ij} is the ratio of image variance at i m spatial resolution to that at j m spatial resolution.

Variance ratio	R^2	P value
Conifers		
R_{12}	0.4128	0.0132
R_{23}	0.4160	0.0128
R_{34}	0.3542	0.0247
R_{45}	0.0665	0.3735
R_{56}	0.0911	0.2944
R_{67}	0.0515	0.4354
Hardwoods		
R_{12}	0.3148	0.1901
R_{23}	0.3972	0.1292
R_{34}	0.2644	0.2377
R_{45}	0.5110	0.0710
R_{56}	0.1820	0.3399
R_{67}	0.1690	0.3595
Conifers and hardwoods		
R_{12}	0.5277	0.0002
R_{23}	0.5446	0.0001
R_{34}	0.5067	0.0003
R_{45}	0.2748	0.0147
R_{56}	0.0606	0.2819
R_{67}	0.0976	0.1679

2×2 to 3×3 m spatial resolutions, while the highest R^2 for hardwoods is at the ratio of 4×4 to 5×5 m. The peak R^2 is greater for hardwoods than for conifers. Similar to table 5, the R^2 values are generally much greater when conifers and hardwoods are pooled. However, the R^2 values for pooled data in table 6 are much lower than those in table 5. Therefore, for pooled data, LAI has a stronger relationship with image variance at a single resolution, while tree crown size has a stronger relationship with the ratio of image variances at two spatial resolutions.

The best relationships between tree crown size or LAI and image spatial properties are shown in figure 3 with conifers and hardwoods pooled. Both tree crown size and LAI are positively related to image variance at 4×4 m spatial resolution, indicating the bigger the tree crown, or the greater the LAI, the greater the image variance. But the relationship between LAI and image variance at 4×4 m spatial resolution (figure 2(*b*)) is much stronger than that between tree crown size and image variance (figure 2(*a*)). The R^2 for using image variance to extract LAI in figure 2(*b*) is much higher than that for using image spectral information (figure 3) and is relatively high compared to other studies in the literature that use image spectral information to estimate LAI. For example, Chen and Cihlar (1996) used normalized difference vegetation index (NDVI) from Landsat TM imagery to extract LAI with an R^2 of 0.38 to 0.52 and Colombo *et al.* (2003) used NDVI from an Ikonos image to estimate LAI with an R^2 of 0.33 when all the vegetation types

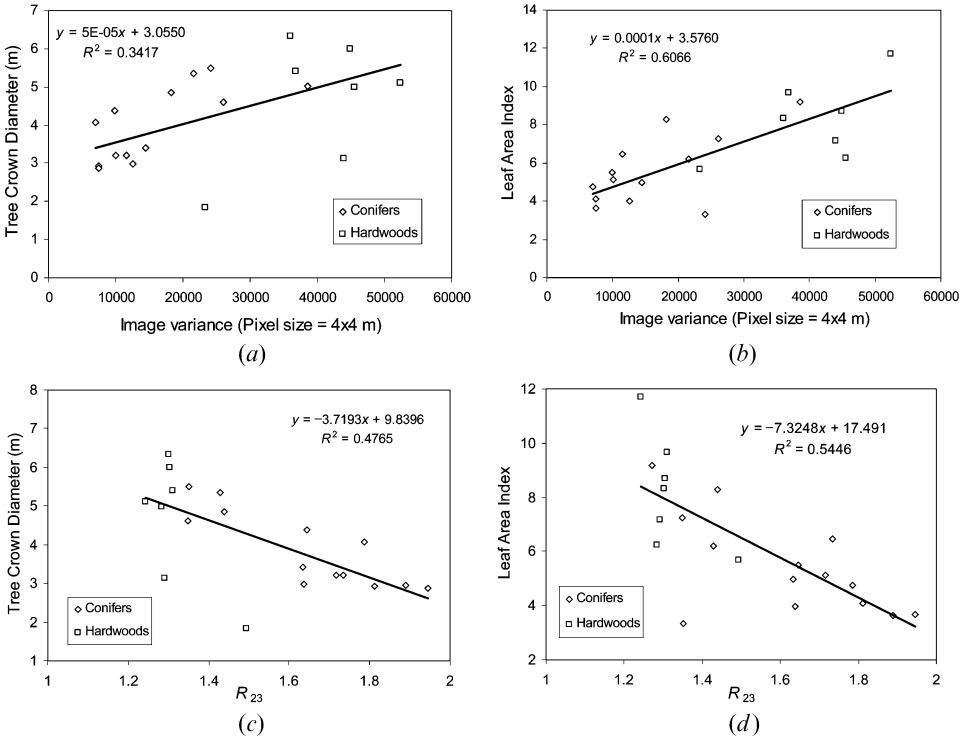

Figure 2. Relationships between image spatial information and canopy structural parameters for pooled conifer and hardwood stands: (*a*) tree crown size versus image variance at 4×4 m spatial resolution, (*b*) LAI versus image variance at 4×4 m spatial resolution, (*c*) tree crown size versus ratio of image variances at 2×2 to 3×3 m spatial resolutions and (*d*) LAI versus ratio of image variances at 2×2 to 3×3 m spatial resolutions.

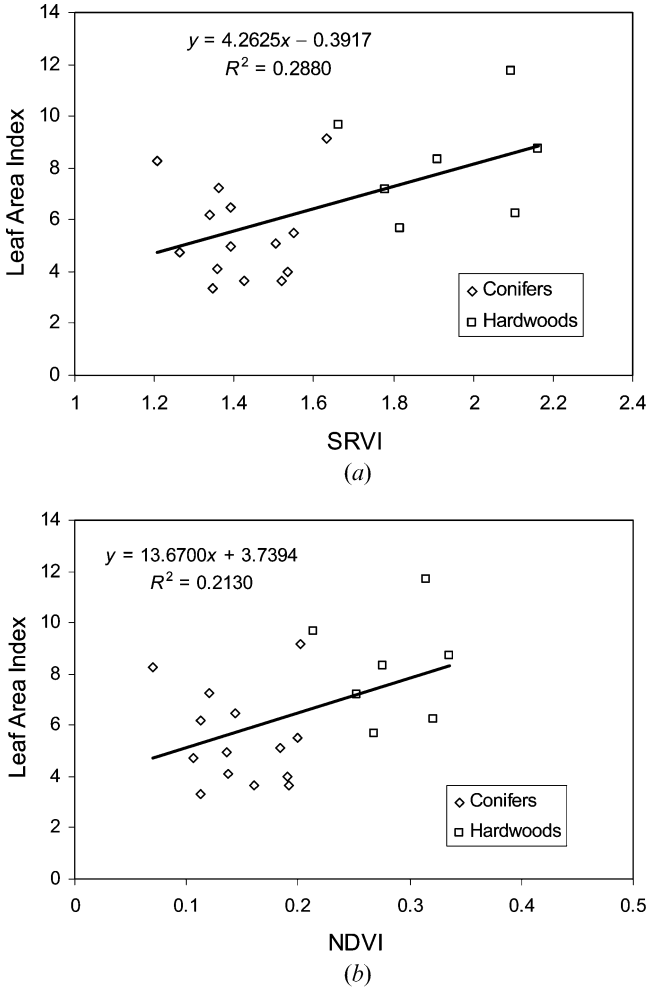

Figure 3. Relationships between spectral vegetation indices and LAI: (*a*) SRVI and (*b*) NDVI. Diamonds (◇) indicate conifer and squares (□) indicate hardwood dominated stands.

were pooled. More recently, Soudani *et al.* (2006) used NDVI from an Ikonos image to estimate LAI with an R^2 of 0.58 (r reported as 0.76 in the original paper) when 28 conifer and hardwood plots were pooled. The usefulness of image spatial information in extracting LAI arises from its insensitivity to the additive or proportional shift of the remotely sensed data (le Maire *et al.* 2006).

In contrast to image variance, tree crown size and LAI are negatively correlated with the ratio of image variances at 2×2 to 3×3 m spatial resolutions. The bigger the tree crown size or the greater the LAI, the smaller the ratio is. This is due to the fact that the image variance decreases at a slower rate when the trees are big than when the trees are small (Song and Woodcock 2003), leading to a lower ratio for stands with bigger trees. When the conifer and hardwood plots are pooled, the relationship of tree crown size with the ratio of image variances at 2×2 to 3×3 m spatial resolutions (figure 2(*c*)) is much poorer than for the conifers alone (table 3). The poor relationship in figure 2(*c*) seems to be due to one hardwood stand, but we cannot discard the stand as an outlier based on the information we have. Careful

examination of figure 2(*c*) found that all the hardwood plots are nearly stacked vertically, indicating that the ratio of image variances does not separate hardwood stands of different crown sizes. Although image variance ratio estimates LAI better than tree crown size when the conifer and hardwood stands are pooled, image variance at 4×4 m spatial resolution estimates LAI much better. Even though image spatial information does not separate tree crown sizes well for hardwoods, it provides a good estimate for LAI, indicating a difference in the scale of spatial variability between tree crown size and LAI.

We classified stands into conifer and hardwood based on basal area in table 2, but we actually only have two pure hardwood stands. All other plots have varying mixtures of conifers and hardwoods. The forests in the study area are almost always mixed stands, while pure conifer or hardwood stands are exceptions. Therefore, it is almost impossible for us to extract LAI for conifers and hardwoods separately. It is encouraging to find that the relationship between LAI and image variance is strengthened when conifers and hardwoods are pooled. However, it remains a challenge to extract tree crown size continuously with high spatial resolution remotely sensed imagery over landscapes with a large hardwood component.

3.3 *Combining spatial and spectral information in extracting LAI*

The NDVI and the simple ratio vegetation index (SRVI) are the most commonly used spectral indices for extracting LAI (Chen and Cihlar 1996, Turner *et al.* 1999, Eklundh *et al.* 2001, Colombo *et al.* 2003, Soudani *et al.* 2006). However, both indices have potential problems because of signature saturation, i.e. the index may no longer respond to increases in LAI when the LAI is high (Fassnacht *et al.* 1997, Turner *et al.* 1999).

Figure 3 shows the relationships between LAI and NDVI and SRVI that we found in this study. Similar to that found in the literature (Chen and Cihlar 1996, Turner *et al.* 1999), the SRVI predicts LAI better than the NDVI. However, if we separate the relationships of LAI with spectral signatures for conifers and hardwoods, the relationship for either would be extremely poor. The relationship is strengthened when the conifer and hardwood stands are pooled, perhaps because of the increased range of LAI. This result is quite different from Colombo *et al.* (2003) who found that the relationships between the NDVI and LAI are strengthened when different types of vegetation are considered separately. But the R^2 values between the NDVI and LAI for forest in Colombo *et al.* (2003) are lower than that for all vegetation types considered together.

The R^2 values between LAI and the spectral indices in figure 3 are much lower than those based on spatial information in table 5. Thus, we further explored the potential in combining both the spectral and spatial information in predicting LAI. Table 7 shows the R^2 values for multiple regressions of LAI with the NDVI and image variance at single spatial resolution, and table 8 shows R^2 values for multiple regressions of LAI with the NDVI and the ratio of image variances at two spatial resolutions. The relationships of LAI with the NDVI and image variances are statistically significant at 95% confidence level for conifers at all spatial resolutions examined, but not significant for hardwoods at the same spatial resolutions. The relationships are significantly strengthened when the conifers and hardwoods are combined (table 7). However, the relationships of LAI with the NDVI and the ratio of image variances at two spatial resolutions are not significant either for conifers or hardwoods, but significant when the conifers and hardwoods are combined. The R^2

Table 7. Results of multiple regression analysis between the LAI and NDVI and image variances at different spatial resolutions. The regression equation is $LAI = b_0 + b_1(NDVI) + b_2 C_{Zi}$, where C_{Zi} is the image variance at i m spatial resolution.

Image variance	R^2	P value
Conifers		
C_{Z1}	0.4221	0.0490
C_{Z2}	0.4441	0.0396
C_{Z3}	0.4500	0.0373
C_{Z4}	0.4648	0.0321
C_{Z5}	0.4231	0.0486
C_{Z6}	0.4573	0.0347
Hardwoods		
C_{Z1}	0.3937	0.3677
C_{Z2}	0.4060	0.3528
C_{Z3}	0.4431	0.3101
C_{Z4}	0.4199	0.3366
C_{Z5}	0.4679	0.2831
C_{Z6}	0.3478	0.4253
Conifers and hardwoods		
C_{Z1}	0.5967	0.0003
C_{Z2}	0.6090	0.0002
C_{Z3}	0.6216	0.0002
C_{Z4}	0.6259	0.0001
C_{Z5}	0.6203	0.0002
C_{Z6}	0.6083	0.0002

Table 8. Results of multiple regression analyses between LAI and NDVI and the ratio of image variances at two spatial resolutions. The regression equation is $LAI = b_0 + b_1(NDVI) + b_2 R_{ij}$, where R_{ij} is the ratio of image variance at i m spatial resolution to that at j m spatial resolution.

Variance ratio	R^2	P value
Conifers		
R_{12}	0.4131	0.0534
R_{23}	0.4169	0.0515
R_{34}	0.3663	0.0814
R_{45}	0.0774	0.6420
R_{56}	0.1056	0.5413
R_{67}	0.0587	0.7170
Hardwoods		
R_{12}	0.3453	0.4287
R_{23}	0.4125	0.3451
R_{34}	0.2854	0.5107
R_{45}	0.5172	0.2331
R_{56}	0.1826	0.6681
R_{67}	0.1692	0.6902
Conifers and hardwoods		
R_{12}	0.5463	0.0008
R_{23}	0.5639	0.0006
R_{34}	0.5350	0.0010
R_{45}	0.3481	0.0213
R_{56}	0.2456	0.0791
R_{67}	0.2986	0.0411

values in table 7 are higher than those in table 8, indicating that image variances are more useful in estimating LAI than ratios of image variances. Compared to using spatial information alone (tables 5 and 6), there is some improvement in R^2 when spatial information is combined with spectral information (tables 7 and 8).

We also examined the benefit of combining the SRVI with spatial information for extracting LAI. The combination of the SRVI with spatial information also leads to some improvement in extracting LAI (results not shown). However, the value of image spatial information is much greater than that of spectral information in extracting LAI. Colombo *et al.* (2003) also found a significant improvement in predicting LAI when the spatial information of a window-based dissimilarity index was included with spectral information.

4. Conclusions

The spatial properties of Ikonos panchromatic imagery are highly informative for both tree crown size and LAI. For conifer and hardwood mixed stands, mean stand tree crown size is most sensitive to the ratio of image variances at 2×2 to 3×3 m spatial resolutions. The LAI for mixed stands is most sensitive to image variance at 4×4 m spatial resolution and it is less sensitive to change in spatial resolution than tree crown size. In addition, image spatial information is more useful for extracting tree crown size for conifer stands than for hardwood stands. However, the relationship between the image spatial information and LAI is stronger when the conifer and hardwood stands are pooled than when they are separated. Compared to the spectral indices of NDVI and SRVI, image spatial information at high spatial resolution is more useful in extracting LAI. Therefore, future efforts to extract LAI from high resolution optical imagery should make use of image spatial information.

Acknowledgements

This research was partly supported by NSF grant 0351430, USDA Forest Service Agenda 2020 and NASA grant NNX06AE28G. The initial manuscript was completed while C. S. was a Charles Bullard Fellow in Forest Research at Harvard Forest, Harvard University from 01 September 2005 to 31 May 2006. The authors acknowledge the assistance from three undergraduate interns for field data collection during the summer of 2005: Ms Andrea Nifong, Ms Elizabeth Ward and Mr Bo Xiao.

References

Asner, G.P., Palace, M., Keller, M., Pereira, R., Silva, J.N.M. and Zweede, J.C., 2002, Estimating canopy structure in an Amazon Forest from laser range finder and IKONOS satellite observations. *Biotropica*, **34**, pp. 483–492.

Barclay, H.J. and Goodman, D., 2000, Conversion of total to projected leaf area index in conifer. *Canadian Journal of Botany*, **78**, pp. 447–454.

Burton, A.J., Pregitzer, K.S. and Reed, D.D., 1991, Leaf-area and foliar biomass relationships in northern hardwood forests located along an 800 km acid deposition gradient. *Forest Science*, **37**, pp. 1041–1059.

Chen, J.M. and Cihlar, J., 1996, Retrieving leaf area index of boreal conifer forests using Landsat TM images. *Remote Sensing of Environment*, **55**, pp. 153–162.

Chen, J.M., Rich, P.M., Gower, S.T., Norman, J.M. and Plummer, S., 1997, Leaf area index of boreal forests: theory, techniques, and measurements. *Journal of Geophysical Research Atmospheres*, **102**, pp. 29, 429, 443.

Clark, D.B., Read, J.M., Clark, M.L., Cruz, A.M., Dotti, M.F. and Clark, D.A., 2004, Application of 1-M and 4-M resolution satellite data to ecological studies of tropical rain forests. *Ecological Applications*, **14**, pp. 61–74.

Cohen, W.B., Spies, T.A. and Fiorella, M., 1995, Estimating the age and structure of forests in a multi-ownership landscape of western Oregon, USA. *International Journal of Remote Sensing*, **16**, pp. 721–746.

Cohen, W.B., Maiersperger, T.K., Yang, Z.Q., Gower, S.T., Turner, D.P., Ritts, W.D., Berterretche, M. and Running, S.W., 2003, Comparisons of land cover and LAI estimates derived from ETM plus and MODIS for four sites in North America: a quality assessment of 2000/2001 provisional MODIS products. *Remote Sensing of Environment*, **88**, pp. 233–255.

Colombo, R., Bellingeri, D., Faolini, D. and Marino, C.M., 2003, Retrieval of leaf area index in different vegetation types using high resolution satellite data. *Remote Sensing of Environment*, **86**, pp. 120–131.

Eklundh, L., Harrie, L. and Kuusk, A., 2001, Investigating relationships between Landsat ETM plus sensor data and leaf area index in a boreal conifer forest. *Remote Sensing of Environment*, **78**, pp. 239–251.

Fassnacht, K.S., Gower, S.T., MacKenzie, M.D., Mordheim, E.V. and Lillesand, T.M., 1997, Estimating the leaf area index of north central Wisconsin forests using the Landsat Thematic Mapper. *Remote Sensing of Environment*, **61**, pp. 229–245.

Franklin, J. and Strahler, A.H., 1988, Invertible canopy reflectance modeling of vegetation structure in semi-arid woodland. *IEEE transactions on Geoscience and Remote Sensing*, **26**, pp. 809–825.

Franklin, S.E., Wulder, M.A. and Gerylo, G.R., 2001, Texture analysis of IKONOS panchromatic data for Douglas-fir forest age class separability in British Columbia. *International Journal of Remote Sensing*, **22**, pp. 2627–2632.

Gower, S.T. and Norman, J.M., 1991, Rapid estimation of leaf-area index in conifer and broad-leaf plantations. *Ecology*, **72**, pp. 1896–1900.

Hurtt, G., Xiao, X.M., Keller, M., Palace, M., Asner, G.P., Braswell, R., Brondizio, E.S., Cardoso, M., Carvalho, C.J.R., Fearon, M.G., Guild, L., Hagen, S., Hetrick, S., Moore, B., Nobre, C., Read, J.M., Sa, T., Schloss, A., Vourlitis, G. and Wickel, A.J., 2003, IKONOS imagery for the large scale biosphere–Atmosphere experiment in Amazonia (LBA). *Remote Sensing of Environment*, **88**, pp. 111–127.

Jenkins, J.C., Chojnacky, D.C., Heath, L.S. and Birdsey, R.A., 2004, *Comprehensive database of diameter-based biomass regressions for North America tree species*, USDA Forest Service, General technical report NE-319.

Jupp, D.L.B., Strahler, A.H. and Woodcock, C.E., 1988, Auto-correlation and regularization in digital images: 1. Basic theory. *IEEE Transactions on Geoscience and Remote Sensing*, **26**, pp. 463–473.

Jupp, D.L.B., Strahler, A.H. and Woodcock, C.E., 1989, Autocorrelation and regularization in digital images: 2. Simple image models. *IEEE transactions on Geoscience and Remote Sensing*, **26**, pp. 463–473.

Kayitakire, F., Hamel, C. and Defourny, P., 2006, Retrieving forest structure variables based on image texture analysis and IKONOS-2 imagery. *Remote Sensing of Environment*, **102**, pp. 390–401.

Knyazikhin, Y., Martonchik, J.V., Myneni, R.B., Diner, D.J. and Running, S.W., 1998, Synergistic algorithm for estimating vegetation canopy leaf area index and fraction of absorbed photosynthetically active radiation from MODIS and MISR data. *Journal of Geophysical Research Atmospheres*, **103**, pp. 32 257–32 275.

Kucharik, C.J., Norman, J.M. and Gower, S.T., 1999, Characterization of radiation regimes in nonrandom forest canopies: theory, measurements, and a simplified modeling approach. *Tree Physiology*, **19**, pp. 695–706.

LE MAIRE, G.L., FRANCOIS, C., SOUDANI, K., DAVI, H., DANTEC, V.L., SAUGIER, B. and DUFRENE, E., 2006, Forest leaf area index determination: a multiyear satellite-independent method based on within-stand normalized difference vegetation index spatial variability. *Journal of Geophysical Research*, **111**, G02027.

LI, X. and STRAHLER, A.H., 1985, Geometric-optical modeling of a conifer forest canopy. *IEEE Transactions on Geoscience and Remote Sensing*, **GE-23**, pp. 705–721.

MONTHEITH, J.L. and UNSWAOTH, M.H., 1973, *Principles of Environmental Physics*, 2nd ed. (London: Edward Arnold).

MYNENI, R.B., HOFFMAN, S., KNYAZIKHIN, Y., PRIVETTE, J.L., GLASSY, J., TIAN, Y., WANG, Y., SONG, X., ZHANG, Y., SMITH, G.R., LOTSCH, A., FRIEDL, M., MORISETTE, J.T., VOTAVA, P., NEMANI, R.R. and RUNNING, S.W., 2002, Global products of vegetation leaf area and fraction absorbed PAR from year one of MODIS data. *Remote Sensing of Environment*, **83**, pp. 214–231.

NI, W., LI, X., WOODCOCK, C.E., BOUJEAN, J. and DAVIS, R.E., 1997, Transmission of solar radiation in boreal conifer forests: measurements and models. *Journal of Geophysical Research*, **102**, pp. 29 555–29 566.

PEDDLE, D.R., BRUNKE, S.P. and HALL, F.G., 2001, A comparison of spectral mixture analysis and ten vegetation indices for estimating boreal forest biophysical information from airborne data. *Canadian Journal of Remote Sensing*, **27**, pp. 627–635.

RUNNING, S.W. and HUNT, E.R. JR., 1993, Generalization of forest ecosystem process model for other biomes, BIOME-BGC, and an application for global-scale models. In *Scaling Physiological Processes: Leaf to Globe*, J.R. Ehleringer and C.B. Field (Eds) (San Diego, CA: Academic Press).

SONG, C., 2004, Cross-sensor calibration between Ikonos and Landsat ETM+ for spectral mixture analysis. *IEEE Geoscience and Remote Sensing Letters*, **1**, pp. 272–276.

SONG, C., 2007, Estimating tree crown size with spatial information of high resolution optical remotely sensed imagery. *International Journal of Remote Sensing*, **28**, pp. 3305–3322.

SONG, C. and BAND, L.E., 2004, MVP: a model to simulate the spatial patterns of photosynthetically active radiation under discrete forest canopies. *Canadian Journal of Forest Research*, **34**, pp. 1192–1203.

SONG, C. and WOODCOCK, C.E., 2003, Estimating tree crown size from multiresolution remotely sensed imagery. *Photogrammetric Engineering and Remote Sensing*, **69**, pp. 1263–1270.

SOUDANI, K., FRANCOIS, C., LE MAIRE, G.L., LE DANTEC, V. and DUFRENE, E., 2006, Comparative analysis of IKONOS, SPOT, and ETM+ data for leaf area index estimation in temperate coniferous and deciduous forest stands. *Remote Sensing of Environment*, **102**, pp. 161–175.

STENBERG, P., RAUTIAINEN, M., MANNINEN, T., VOIPIO, P. and SMOLANDER, H., 2004, Reduced simple ratio better than NDVI for estimating LAI in Finnish pine and spruce stands. *Silva Fennica*, **38**, pp. 3–14.

THORNTON, P.E., 2000, *Biome-BGC Version* 4.1.1, Numerical Terradynamics Simulation Group (NTSG), School of Forestry, University of Montana, Missoula, MT 59812.

TURNER, D.P., COHEN, W.B., KENNEDY, R.E., FASSNACHT, K.S. and BRIGGS, J.M., 1999, Relationships between leaf area index and Landsat TM spectral vegetation indices across three temperate zone sites. *Remote Sensing of Environment*, **70**, pp. 52–68.

WELLES, J.M. and NORMAN, J.M., 1991, Instrument for indirect measurement of canopy architecture. *Agronomy Journal*, **83**, pp. 818–825.

WHITE, J.D., RUNNING, S.W., NEMANI, R., KEANE, R.E. and RYAN, K.C., 1997, Measurement and remote sensing of LAI in Rocky Mountain montane ecosystems. *Canadian Journal of Forest Research*, **27**, pp. 1714–1727.

WOODCOCK, C.E. and STRAHLER, A.H., 1987, The factor of scale in remote sensing. *Remote Sensing of Environment*, **21**, pp. 311–332.

WOODCOCK, C.E., COLLINS, J.B., JAKABHAZY, V.D., LI, X., MACOMBER, S.A. and WU, Y., 1997, Inversion of the Li–Strahler canopy reflectance model for mapping forest structure. *IEEE Transactions on Geoscience and Remote Sensing*, **35**, pp. 405–414.

WOODCOCK, C.E., COLLINS, J.B., GOPAL, S., JAKABHAZY, V.D., LI, X., MACOMBER, S.A., RYHERD, S., HARWARD, V.J., LEVITAN, J., WU, Y. and WARBINGTON, R., 1994, Mapping forest vegetation using Landsat TM imagery and a canopy reflectance model. *Remote Sensing of Environment*, **50**, pp. 240–254.

WU, Y. and STRAHLER, A.H., 1994, Remote estimation of crown size, stand density and biomass on the Oregon transect. *Ecological Applications*, **4**, pp. 299–312.

WULDER, M.A., LEDREW, E.F., FRANKLIN, S.E. and LAVIGNE, M.B., 1998, Aerial image texture information in the estimation of northern deciduous and mixed wood forest leaf area index (LAI). *Remote Sensing of Environment*, **64**, pp. 64–76.